Trigger logic of the ATLAS First Level Muon Trigger

R.Cardarelli, F.Ceradini, N.Filippini, E.Gennari,
A.Nisati, E.Petrolo, R.Santonico, S.Veneziano
INFN, Dipartimento di Fisica,
Universitá di Roma La Sapienza, Rome Italy
R.Bindra, B.Claxton, J.Dowdell, A.Letchford, S.Quinton
Rutherford Appleton Laboratory, UK
N.Ellis
CERN, Switzerland

October 9, 1995

Abstract

We present the design of the first level muon trigger in the central toroid of the ATLAS experiment at the Large Hadron Collider (LHC). The trigger is based on fast, finely segmented gaseous detector, Resistive Plate Chambers (RPC), to unambigously identify the interaction bunch crossing and to provide a sharp threshold over a large interval of transverse momentum. We describe the logic scheme of the trigger and the performance of the local trigger logic we have realized.

1 Introduction

The quality of the muon spectrometer will be one of the keys of ATLAS discovery potential [1]. The muon spectrometer design emphasises reliable, high-resolution, standalone performance over a p_T range from 5 to about 1000 GeV/c. The high quality spectrometer has to be complemented with matching trigger capabilities. The physics programme requires detection of muons from semileptonic decays of heavy quarks down to 5 GeV/c. For physics signals involving the detection of intermediate vector bosons a p_T threshold at 20 GeV/c is adequate. Precision momentum measurement and triggering are done by two dedicated detectors; the trigger chambers also provide the second coordinate measurement and timing information to relate muon tracks to bunch crossings of period $T = 25\ ns$. The low-energy charged and neutral particles flux at the LHC will be fairly high [7]. These backgrounds have a major impact on the trigger rate and pattern recognition efficiency.

2 Trigger system

The transverse momentum selection is done with a fast coincidence between strips on different planes. The number of trigger planes is defined by the need to minimize the rate of accidental coincidences and to optimize the efficiency. To reduce the accidental rate to a level lower than the prompt muon rate, the trigger will operate in two projections, $r - z$ and $r - \phi$. Thus the trigger detectors will also be used to provide the coordinate in the non-bending plane ($r - \phi$) to the muon tracking system.

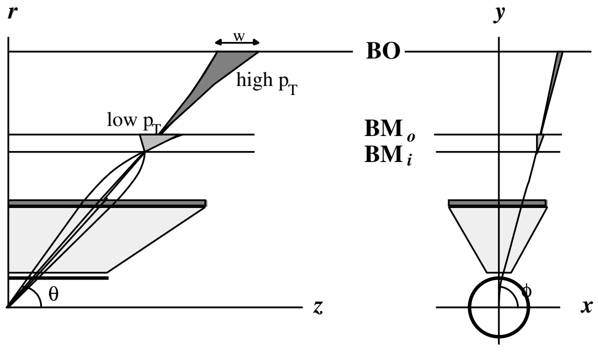

Figure 1: Scheme of the first-level muon trigger in the barrel

The different momentum selection criteria required by the relevant physics processes are best met using a low and a $high - p_T$ trigger. This is implemented in the barrel as shown in Fig.1. The trigger scheme uses three stations, two middle stations (BM), each made of two RPC planes and the outer station (BO), made of three RPC planes.

RPCs are proposed for their good time resolution, easiness in segmentation and low cost of production [3][4]. Each RPC plane will be equipped with read-out strips on either side of the gas volume: z-strips parallel to the magnetic field and ϕ-strips parallel to the beam. The detector will be operated in avalanche mode [2].

The $low - p_T$ trigger requires a three-fold majority of the four middle planes while the $high - p_T$ trigger requires a two-fold majority of the three BO planes in coincidence with the $low - p_T$ trigger. The trigger rate in the barrel is shown in Fig.2 as a function of the luminosity for the low-p_T and high-p_T trigger configurations together with the muon rate.

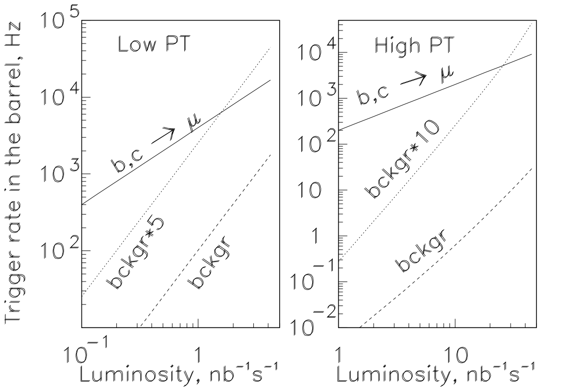

Figure 2: Low and High-p_T trigger rate in $\mid \eta \mid < 1.05$ as a function of the luminosity

The size of the trigger window, to select muons with transverse momentum larger than p_T is $w_{barrel} \simeq a/\rho p_T \sin^2\Theta$, where ρp_T is the value of the transverse momentum after traversing the calorimeter. Fluctuations in the energy loss and multiple scattering in the calorimeter, lenght of the interaction region and non uniformity of the magnetic field are all smearing effects which make the choice of $3 - 4\ cm$ strip pitch a balanced choice between good selectivity and number of channels.

2.1 Trigger segmentation, ROI's

The trigger detectors in the barrel are segmented in 24 ϕ sectors: 16 between the coils (large sectors) and 8 close to the coils (small sectors). Along the z axis the segmentation is projective to the interaction vertex. While the segmentation of the detector itself comes mainly from the geometry of the experiment.

The p_T threshold coming from L1 will be refined at second level trigger (L2), by using the high precision chambers' information. The L1 will provide Regions Of Interest (ROI), where the L2 processor will search for muon tracks in small sectors of the spectrometer. The L2 algorithm is initiated by the L1 strip information that has an average occupancy much smaller than the precision drift chamber. A good compromise between layout considerations and L2 needs is a segmentation $\Delta\eta \times \Delta\phi \sim 0.13 \times 0.10$. In this case the barrel will be equipped with 2304 matrices of 32×64 strips.

3 The Muon trigger processor

To be able to uniquely identify tracks belonging to a bunch crossing, it is not only necessary to have a fast detector, but the trigger electronics itself must have a time resolution comparable to the detector. Moreover the trigger has to be multithreshold, allowing multimuon events to be selected with thresholds lower than the single muon ones. Six thresholds will be programmable in the range $5 - 35\ GeV/c$.

All the previous needs are best met by developing an Application Specific Integrated Circuit (ASIC), which will be mounted locally on the detector, close to the frontend electronics. The gathering of data for the local logic will be done by 48 Sector logic processors, each reading 24 $r - z$ and 24 $r - \phi$ matrix outputs, covering 24 ROIs. The main function of the sector logic is, concentrate L1 data, cluster hits from the same track, associate tracks in the two projections and eliminate double counting of tracks giving hits in two or more ROIs. The Sector logic output will be concentrated to the Global μ trigger through 96 links running at $800\ Mbit/s$. The Global μ trigger will generate total multiplicity for each of the 6 thresholds and send this information to the L1 Main processor at the $40\ MHz$ bunch crossing frequency. In the sector and global μ logic more detailed information will be stored for the ROI builder and via the L2 readout links sent to the L2 buffers. The total expected data rate does not exceed $10\ Mbyte/s$, while the detector data will be around $70\ Mbyte/s$. The total L1 latency is less than $1.5\ \mu s$

3.1 Synchronization

Due to the large area of the detector, timing is a critical issue; propagation time along different regions of the detector, as well particles' time of flight can be longer than T. The ATLAS Timing Control and Distribution System [6], will be used as the starting point by providing a reference $f_B = 40\ MHz$ clock and a programmable bunch crossing number. Finer sub-period delays will be implemented using programmable depth micropipelines, for unique assignment of a track to a bunch crossing. A time interpolator running at $4f_B$ or $8f_B$ frequency will be needed to monitor these delays.

3.2 The coincidence matrix

Our group has realized [5], in collaboration with the Rutherford Laboratory, a $0.5\ \mu m$ CMOS $34k$ gate array for the front-end part of the trigger system.

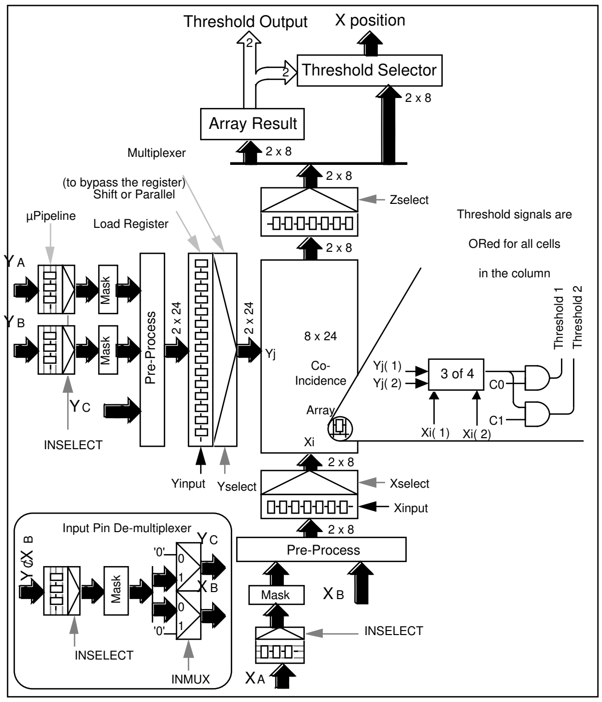

Figure 3: Block diagram of the coincidence matrix ASIC

The demonstrator circuit contains two 8×24 coincidence matrices. The $low - p_T$ and $high - p_T$ algorithm can be implemented programming the same circuit for the two modes of operation. The detector signals, after discrimination, are fed into a micropipeline running at a frequency multiple of $1/T$. This is done to compensate for different propagation times from different detector planes. The 3/4 or 2/3 majority algorithm is done in two steps; one part is common to all the columns or rows of the matrix (Pre-Process blocks), while the other has to be done cell by cell. The (most significant) hit pattern of the muon track(s) is fed into an output register, together with the threshold value the track(s) has (have) passed. The logic is distributed over an internal pipeline of maximum 4 steps lenght. The circuit can operate in fully pipelined mode, fully combinatorial, or any combination of the two. Additional test facilities and the possibility of masking noisy channels or missing planes have been realized within the gate array cell quota. All internal registers are accessed by a dedicated serial input and output lines. The die operates at $3.3\ V$ and is mounted on a 120 pin QFP package. Laboratory tests have proved that the maximum skew between different inputs to different outputs is below $1.8\ ns$, maximum operating frequency is above $100\ MHz$, total processing time in fully combinatorial mode is $\simeq\ 7\ ns$, the same for the two trigger algorithms. A dedicated VME board has been designed for the purpouse of testing the ASIC in a test beam. The board is a 6U VME board with 88 differential ECL inputs (four detector planes) and 16 differential ECL outputs. Two NIM inputs are used for fast clear and for the external clock. Two NIM outputs provide the threshold outputs. The interface between the VMEbus and the ASIC internal registers is realized with an FPGA (Xilinx 3042) which converts parallel longwords into variable lenght serial words and vice versa. The ASIC run mode and clock settings can be changed via this FPGA.

3.3 Beam tests

These circuits have been tested in the H8 test beam at CERN with RPCs illuminated by $180\ GeV/c$ muons.

The trigger hodoscope used seven chambers with orthogonal strip readout to identify muons in two projections, and was arranged in two doublets and a triplet, respectively $40\ cm$ and $200\ cm$ apart. The test trigger system is shown in figure 4. In total eight trigger boards were needed to trigger on both projections and 224 (chambers) + 80 (trigger) channels were digitized by standard $1\ ns$ LSB multihit TDCs. In figure 5 the Time of flight between the two doublets and between the first doublet and the triplets are shown; a $\sigma\ \simeq\ 3\ ns$ is measured.

In figure 6 the time response of the low and high P_t coincidence matrices, is shown for both projections. A processing time of the $high - P_t$ algorithm of $\simeq 13\ ns$

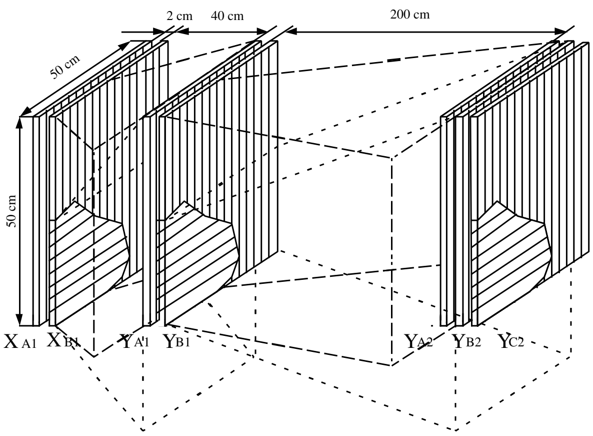

Figure 4: The RPC trigger tower at H8. The dotted lines are regions covered by one matrix

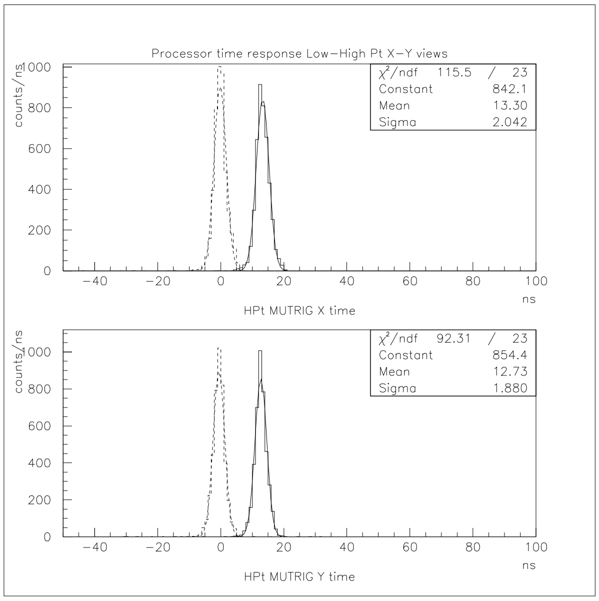

Figure 6: Trigger system time response on the two projections. The dotted line distributions are the $low - p_T$ processor responses while the full line distributions are the $high - p_T$ processors response

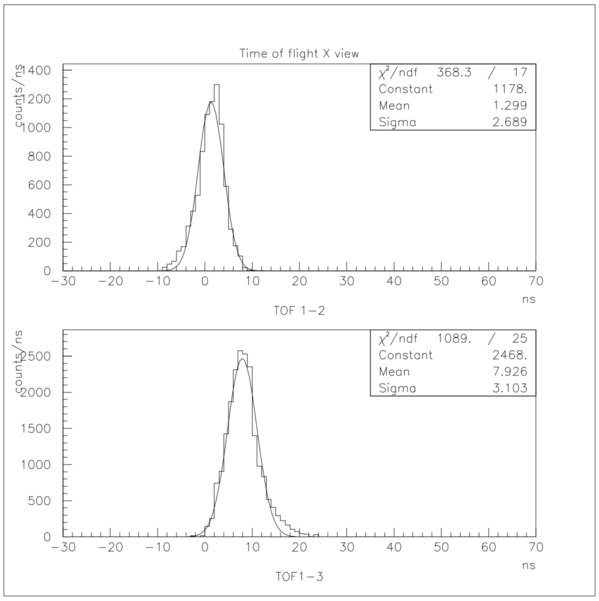

Figure 5: time of flight between the two doublets(top) and the first doublet and the triplet(bottom)

is measured including cables and time of flight. The integrated detector/electronics time resolution is $\simeq 2\ ns$.

4 Conclusions

The ATLAS level 1 muon trigger logic is designed to make unique bunch crossing ID and provide sharp thresholds over a wide range of transverse momenta. The local trigger logic has been succesfully designed and tested, based on a $0.5\ \mu m$ CMOS circuit ($Fujitsu\ CG51$). The ASIC performed as expected. This technology is already mature to fulfill our needs of low propagation time and integration. The final implementation will simply be scaled to a 32×48 coincidence (100k gates required). Faster IO will be used to provide the necessary $160 - 320\ MHz$ needed in the experiment. The current technology already uses differential PECL to drive signals at frequencies in excess of $350\ MHz$.

References

[1] ATLAS
Techn. Prop., CERN/LHCC/94-43, LHCC/P2, 15

December 1994.

[2] G.L.Bencze et al, Nucl. Instr. and Meth. in Phys. A 352(1995) 552-556.

[3] L.Acitelli et al., ”Study of the efficiency and time resolution of a RPC irradiated with photons and neutrons”, prep.1039 Dipartimento di Fisica, Universitá di Roma ”La ”Sapienza,15/7/1994.

[4] G.L.Bencze et al., Nucl. Instr. and Meth. in Phys. A340 (1994)466

[5] J. Dowdell et al., ”A coincidence array demonstrator ASIC for the RD-27 muon trigger”, RD-27 Note 30, July 1994.

[6] B.G. Taylor, IEEE Nucl. Science Symposium, San Francisco, 31/10-6/11 1993.

[7] G.Battistoni, A.Ferrari and P.R.Sala, ”Background calculations for the ATLAS detector and hall”, ATLAS note GEN-NO-010, 13.10.1994.